

A micromachined tunable coupled-cavity laser for wide tuning range and high spectral purity

H. Cai¹, B. Liu¹, X. M. Zhang², A. Q. Liu^{1*}, J. Tamil¹, T. Bourouina³ and Q. X. Zhang⁴

¹*School of Electrical and Electronic Engineering, Nanyang Technological University, Nanyang Avenue, Singapore 639798*

²*Department of Mechanical Engineering, University of Maryland College Park, MD 20742, USA,*

³*ESIEE/Esycos-Lab, cite Descartes 2 Bd Blaise Pascal, 93162, Noisy-le-Grand cedex France,*

⁴*Institute of Microelectronics, 11 Science Park Road, Singapore 117685,*

*Corresponding author: eaqliu@ntu.edu.sg; Tel: (65) 6790-4336, Fax: (65) 6793-3318

Abstract: This paper presents the design and experimental study of a coupled-cavity laser based on the micromachining technology for wide tuning range and improved spectral purity. The core part of this design utilizes a deep-etched movable parabolic mirror to couple two identical Fabry-Pérot chips and thus allows the active adjustment of the cavity gap so as to optimize the mode selection and to increase the tuning range as well. In experiment, the laser achieves the single longitudinal mode output over 51.3 nm and an average side-mode-suppression ratio of 22 dB when the tuning current varies from 5.7 – 10.8 mA. The measured wavelength tuning speed is 1.2 μ s and the single mode output is stable at any wavelength when the tuning current is varied within ± 0.06 mA. Compared with the conventional fixed cavity gap coupled-cavity lasers, such design overcomes the phase mismatching and mode instability problems while maintaining the merit of high-speed wavelength tuning using electrical current.

©2008 Optical Society of America

OCIS codes: (230.4685) Optical microelectromechanical devices; (130.3990) Micro-optical devices; (140.3600) Lasers, tunable; (140.3325) Laser coupling.

References and links

1. E. Bruce, "Tunable lasers," *IEEE Spectrum* **39**, 35-39 (2002).
2. L. A. Coldren, "Monolithic tunable diode lasers," *IEEE J. Sel. Top. Quantum Electron.* **6**, 988-999 (2000).
3. M. C. Y. Huang, Y. Zhou, and C. J. Chang-Hasnain, "A nanoelectromechanical tunable laser," *Nat. Photonics* **2**, 180-184 (2008).
4. N. P. Caponio, M. Goano, I. Maio, M. Meliga G. P. Bava, G. D. Anis, and I. Montrosset, "Analysis and Design criteria of Three-section DBR tunable lasers," *IEEE. J. Sel. Areas Commun.* **8**, 1203-1213 (1990).
5. C. W. Wilmsen, H. Temkin, and L. A. Coldren, *Vertical-Cavity Surface emitting lasers: Design, Fabrication, Characterization, and Applications* (Cambridge Univ. Press, New York, 1999).
6. P. M. Anandarajah, R. Maher, and L. P. Barry, et al., "Characterization of frequency drift of sampled-grating DBR laser module under direct modulation," *IEEE Photon. Technol. Lett.* **20**, 239-241 (2008).
7. Y. Tohmori, Y. Yoshikuni, and H. Ishii, "Broad-range wavelength-tunable superstructure grating (SSG) DBR lasers," *IEEE J. Quantum Electron.* **29**, 1817-1823 (1993).
8. M. C. Y. Huang, Y. Zhou, and C. J. Chang-Hasnain, "A surface-emitting laser incorporating a high-index-contrast subwavelength grating," *Nature Photon.* **1**, 119-122 (2007).
9. M. C. Y. Huang, Y. Zhou, and C. J. Chang-Hasnain, "Nano electro-mechanical optoelectronic tunable VCSEL," *Opt. Express* **15**, 1222-1227, (2007), <http://www.opticsinfobase.org/abstract.cfm?URI=oe-15-3-1222>.
10. L. A. Coldren, B. I. Miller, K. Iga, and J. A. Rentschler, "Monolithic two-section GaInAsP/InP active-optical-resonator devices formed by reactive-ion-etching," *Appl. Phys. Lett.* **38**, 315-317 (1981).
11. W. T. Tsang, N. A. Olsson, and R. A. Logan, "High-speed direct single-frequency modulation with large tuning rate and frequency excursion in cleaved-coupled-cavity semiconductor lasers," *Appl. Phys. Lett.* **42**, 650-652 (1983).
12. L. A. Coldren and T. L. Koch, "Analysis and design of coupled-cavity lasers," *IEEE J. Quantum Electron.* **20**, 659-682 (1984).
13. T. L. Koch and L. A. Coldren, "Optimum coupling junction and cavity length for coupled-cavity semiconductor lasers," *J. Appl. Phys.* **57**, 742-754 (1985).

14. R. J. Lang and A. Yariv, "An exact formulation of coupled-mode theory for coupled-cavity lasers," *IEEE J. Quantum Electron.* **24**, 66-72 (1988).
 15. A. Q. Liu, X. M. Zhang, H. Cai, A. B. Yu, and C. Lu, "Retro-axial VOA using parabolic mirror pair" *IEEE Photon. Technol. Lett.* **19**, 692-694 (2007).
 16. X. M. Zhang, A. Q. Liu, D. Y. Tang and C. Lu, "Discrete wavelength tunable laser using microelectromechanical systems technology," *Appl. Phys. Lett.* **84**, 329-331 (2004)
 17. A. Q. Liu, X. M. Zhang, D. Y. Tang and C. Lu, "Tunable laser using micromachined grating with continuous wavelength tuning," *Appl. Phys. Lett.* **85**, 3684-3686 (2004).
 18. A. Q. Liu, X. M. Zhang, "A review of MEMS external-cavity tunable lasers," *J. Micromech. Microengin.* **17**, R1-R13 (2007).
 19. A. E. Siegman, *Lasers* (University Science Books, CA, 1986).
 20. Y. Sidorin and D. Howe, "Laser-diode wavelength tuning based on butt coupling into an optical fiber," *Opt. Lett.* **22**, 802-804 (1997).
-

1. Introduction

Tunable lasers have been very attractive sources for many applications such as biophysics, spectroscopy, metrology, and optical communications. Although many semiconductor-lasers-based approaches have been explored to realize the ability of wavelength tuning, this important function is still inadequate for their advance and wide applications [1, 2]. Moreover, the limitations in terms of narrow wavelength tuning range and slow tuning speed particularly prevent them from exerting their full potential to many emerging applications [3], such as wavelength-based packet switching and all-optical networks. Monolithically-integrated semiconductor tunable lasers have been extensively studied due to their advantages of compactness, reliability and potentially low cost. However, a conventional monolithic tunable laser comprises a multi-electrode structure including a distributed Bragg reflector (DBR) [4, 5], which increases the complexities and difficulties in fabrication as well as wavelength tuning control. Furthermore, the limitations of optical and thermal properties of candidate DBR materials make it challenging to obtain large wavelength tuning range. On the other hand, more sophisticated tunable lasers with wide tuning ranges have also been developed, such as sampled grating distributed Bragg reflector (SGDBR) lasers [2, 6], superstructure grating (SSG) DBR lasers [7] and high-contrast-subwavelength-grating (HCG) reflector based surface-emitting lasers [8, 9]. In addition to the fabrication difficulties involving gratings and/or multiple epitaxial growths, the requirements to the reflector bandwidth and reflectivity become even more stringent. Therefore, these problems present to be the major obstacles to their wide commercial deployment.

Coupled-cavity laser (CCL) is another option for wavelength tuning. A typical CCL is formed by coupling two or more laser cavities, which can be fabricated by etching a narrow groove inside a cleaved single chip [10] or by employing cleaved-coupled-cavity structures [11]. The dominant oscillation mode of the CCL is determined by the interference of the optical fields in all the optical cavities involved. Tremendous study has been carried out for such CCLs, and the theories have been well established [12-14]. However, it remains a challenge to obtain optimal cavity coupling and phase matching at the same time, especially when the two coupled cavities have fixed cavity gaps as predetermined during the fabrication. The etched cavity gaps have to be finely controlled during the fabrication (otherwise, low yield). Even though, the fixed gap is not adaptive to the variations of working conditions (such as environmental temperature change) and may lead to unstable single-mode operation and limited mode selectivity. These problems have affected the practical applications of the CCLs.

To tackle these problems, we propose in this paper a micromachined CCL configuration using an actively adjustable cavity gap based on the Microelectromechanical Systems (MEMS) technology. The active adjustment of the cavity gap provides optimal phase matching and mode selection while the MEMS technology ensures high compactness and easy integration. In this paper, the design of the micromachined CCL will be presented in Section 2, followed by the theoretical explanations in Section 3. The experimental results and tuning characteristics will be elaborated in Section 4.

2. Design of Micromachined tunable coupled-cavity laser

The design of the micromachined tunable coupled-cavity laser is depicted schematically in Fig. 1. In this design, the micromachined CCL consists of two identical chips (i.e., twin chips) and a micromachined movable parabolic mirror [15]. The two chips both are normal Fabry-Pérot (FP) chips (named as lasing chip and tuning chip). They are optically coupled through the parabolic mirror but electrically isolated. In this case, two sets of electrodes are available for the FP chips, one for a constant current (above the threshold) injected to the lasing chip and the other for a variable current (below the threshold) applied to the tuning chip. Therefore, each chip has independent electrical control. According to the operation principle of the CCL (to be discussed below), there is an optimal cavity gap length between the two chips in order to obtain a stable single-mode output with high spectral purity. The movable parabolic mirror is designed to optimize the cavity gap. It should be noted no further mirror movement is required once the stable single mode output is achieved. The wavelength tuning is achieved by varying the driving current of the tuning chip, not by moving the mirror. In this way, the wavelength tuning speed is not limited by the mechanical response, as opposite to many developed micromechanical tunable lasers [16-18].

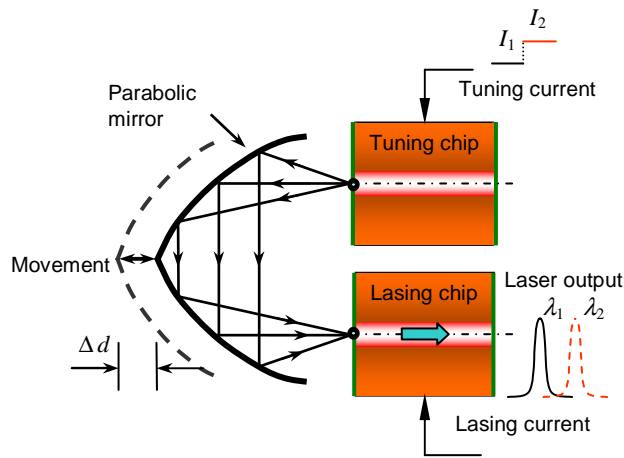


Fig. 1. Schematic diagram of micromachined tunable coupled-cavity laser.

The parabolic mirror is a symmetrically arranged pair of parabolic parts, whose foci are positioned at the two adjacent facets of the chips, respectively. Based on the geometric optics, the beams from the focus point of a parabola are collimated by the parabolic surface, and vice versa. Therefore, the parabolic mirror provides optical coupling for the micromachined CCL. Due to the deep-etching process, the mirror is actually 2-dimensional and has the focusing/collimation effect only in the horizontal plane, nevertheless it provides sufficient coupling. In addition, the coupling efficiency is insensitive to the horizontal translation of the mirror, as confirmed in a recent study [15].

3. Theoretical analysis

3.1 Wavelength tunability

The basic principle of the micromachined CCL is illustrated schematically in Fig. 2. According to the resonance condition of the optical cavity, a set of potential longitudinal modes of the lasing chip (FP cavity) of the micromachined CCL can be defined as [2]:

$$\lambda_N = \frac{2n_{\text{eff}}L}{N} \quad (1)$$

where λ_N is the longitudinal mode wavelength, which is essentially reciprocal to the corresponding mode number N , n_{eff} denotes the effective group refractive index of the FP cavity, and L is the cavity length.

Subsequently, the comb-mode spectrum of the lasing chip has an almost constant mode spacing ($\Delta\lambda_1$), which is give by:

$$\Delta\lambda_1 = \frac{\lambda_0^2}{2n_{eff1}L_1} \quad (2)$$

Where λ_0 is the wavelength in vacuum, n_{eff1} represents the effective group refractive index. L_1 is the cavity length of the lasing chip.

Similarly, the mode spacing ($\Delta\lambda_2$) of the tuning chip can be expressed as:

$$\Delta\lambda_2 = \frac{\lambda_0^2}{2n_{eff2}L_{eff2}} = \frac{\lambda_0^2}{2(n'_{eff2}L_2 + n_{air}d)} \quad (3)$$

where n_{eff2} and L_{eff2} represent the effective group refractive index and the cavity length of the combined tuning cavity, respectively. L_2 is the cavity length of tuning chip, n_{air} represents the air refractive index and d is the cavity gap distance between the two chips. As different driving current results in different effective group refractive index, the mode spacings of the two FP chips are different even though they have the same cavity length.

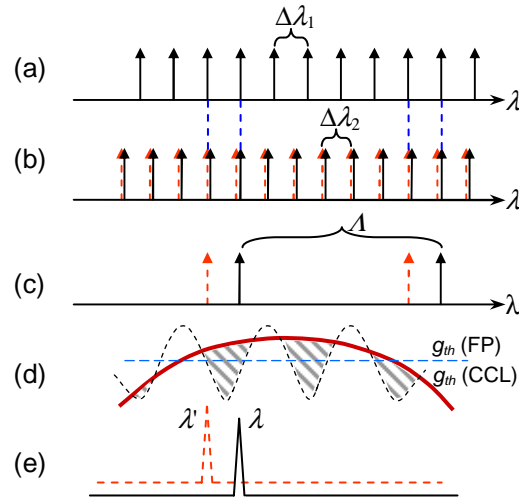


Fig. 2. Mechanism of the wavelength tuning in the coupled-cavity laser, the solid and dashed lines correspond to the different injection current applied to the tuning chip. (a). Possible modes of the lasing chip; (b). possible modes of the tuning chip; (c). coincident modes of the coupled-cavity; (d). laser gain profile; and (e). coupled-cavity laser output spectrum.

The lasing mode of the micromachined CCL is determined by the coincidence of the two modes from lasing chip and tuning chip, respectively. The lasing chip has evenly distributed modes with a mode spacing of $\Delta\lambda_1$ as shown in Fig. 2(a) and similarly the tuning chip has a mode spacing of $\Delta\lambda_2$ as shown in Fig. 2(b). When the two cavities are optically coupled with a specific cavity gap d but the mode spacings $\Delta\lambda_1$ and $\Delta\lambda_2$ are slightly different, the spectral spacing (Λ) of the neighboring enforced/aligned mode is given approximately by [11]:

$$\Lambda = \frac{\Delta\lambda_1 \cdot \Delta\lambda_2}{|\Delta\lambda_1 - \Delta\lambda_2|} = \frac{\lambda_0^2}{2|n_{eff1}L_1 - n_{eff2}L_{eff2}|} \quad (4)$$

It is noticed that Λ can be significantly larger than either of the original individual FP chip mode spacing (see Fig. 2(c)) when the difference between $n_{eff2}L_{eff2}$ and $n_{eff1}L_1$ is small enough. If Λ is generally larger than the spectral width of the laser gain window (Fig. 2(d)), it allows only one coincident mode to oscillate as shown in Fig. 2(e). In other words, the coincident mode interferes constructively and becomes the enforced/aligned mode of the micromachined CCL, while all the other modes interfere destructively and become suppressed.

During the wavelength tuning operation, the lasing chip provides the potential modes while the tuning chip selects one mode to oscillate. The tuning current applied to the tuning chip causes a change of the effective refractive index by the free carrier plasma effect. Therefore, there is a wavelength shift in $\Delta\lambda_2$. The original coincident mode is thus misaligned and the adjacent mode becomes matched. As a result, the laser output wavelength is tuned. Since the wavelength tuning is realized by the free carrier plasma effect in the tuning chip, the tuning speed is expected at the level of micro-seconds or even nano-seconds [12].

3.2 Equivalent model and threshold conditions

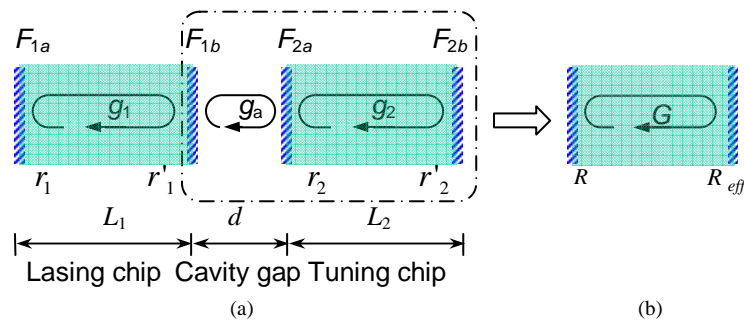


Fig. 3. Analytical model of micromachined coupled-cavity laser. (a) Two Fabry-Pérot cavities based coupled-cavity model; and (b) simplified equivalent single-cavity model

A simplified micromachined CCL model is shown in Fig. 3(a). It consists of two FP chips separated by an air gap (i.e. cavity gap). F_{1a} , F_{1b} , F_{2a} and F_{2b} denote the facets of two FP chips (1 refers to lasing chip, and 2 refers to tuning chip). r_1 , r'_1 , r_2 and r'_2 are the reflectances of F_{1a} , F_{1b} , F_{2a} and F_{2b} , respectively. g_1 , g_{air} and g_2 describe the roundtrip gains inside the cavities of the lasing chip, the cavity gap and the tuning chip, respectively. L_1 , L_2 and d are the corresponding chip cavity length/ cavity gap distance. The micromachined CCL configuration can be further simplified into a single-cavity scheme as shown in Fig. 3(b), where R is the reflectance of F_a ($R = r_1$), G describes the roundtrip gain inside the lasing chip ($G = g_1$). The effective reflectance of the equivalent cavity, R_{eff} is given by [19, 20]:

$$R_{eff} = \frac{r'_1 (1 - r_2 r'_2 g_2) - g_{air} (r_2 - r'_2 g_2)}{1 - r'_1 r_2 g_{air} - r_2 r'_2 g_2 + r'_1 r'_2 g_{air} g_2} \quad (5)$$

where the roundtrip gain within the cavity gap is given by $g_{air}(d, \lambda) = \exp(-2\alpha_{air}d - j4\pi d/\lambda)$, α_{air} and λ denote the optical loss coefficient and wavelength, respectively. Similarly, the roundtrip gain within the tuning cavity is given by $g_2(n_2, \lambda) = \exp(-2\alpha_2 n_2 L_2 - j4\pi n_2 L_2/\lambda)$, α_2 and n_2 denote the absorption coefficient and the refractive index of the tuning chip, respectively. With this effective reflectivity (R_{eff}), the lasing chip of the micromachined CCL is modulated as the function the refractive index of the tuning chip (n_2) and the distance of the cavity gap (d). Therefore, the gain condition for micromachined CCL lasing can be expressed as [20]:

$$g(d, n_2, \lambda) = \alpha_m - \ln |R_{eff}(d, n_2, \lambda)| / L_1 \quad (6)$$

where α_m is the internal loss of the lasing cavity and \ln represents the natural logarithm. By varying injection current to the tuning chip, its refractive index (n_2) is changed. As a result, the gain of the micromachined CCL is modulated. Figure 4 illustrates the threshold gain modulation introduced by the effective reflectivity R_{eff} . As shown in Fig. 4(a), the periodical property of the threshold gain (solid line) is determined by the cavity length of the tuning chip, while the air cavity gap controls the bottom envelop (dash line). Only the wavelengths falling on the bottom envelope and covered by the shadow are the possible oscillating modes which are strongly supported by the tuning cavity. Among those modes, the one which can match the lasing cavity supporting mode will be the final lasing mode of the micromachined CCL, with the condition of lower threshold gain required (see Fig. 2(d)). When the air cavity gap is set to an optimal distance (i.e. $d = d_0$), there is only one of matching modes falling in the “ shadow window” , which will be the single mode lasing output. Otherwise, an unsuitable gap (i.e. $d \neq d_0$) provides several “ shadow windows” at the same time, which causes any matching modes loading in these windows to be one of the outputs. Such unsuitable gap results in multi-mode and unstable output. Consequently, an optimal cavity gap enhances the tunability and selectivity of the micromachined CCL. On the other hand, the change of the tuning current (ΔI) introduces a variation in the refractive index (Δn_2), which results in a shift of the threshold, as shown in Fig. 4(b). During the operation of the micromachined CCL, the tuning chip introduces an optical feedback (powered by its cavity gain medium) to the lasing chip, causing the cavity gain ($g_{th(CCL)}$), as given by Eq. 6) to be highly modulated. Particularly, with the adjustable cavity gap, it widens up the “cavity gain window”, as indicated with shadow in Fig. 2(d). Hence, this modulation is the key to obtaining a large tuning range. In addition, it enhances the mode selectivity, which is related to the side-mode suppression ratio (SMSR). Based on the above analyses on wavelength tunability and the threshold condition, we can see that the tuning current not only causes wavelength tuning but also improves the wavelength tuning range and mode selectivity. Once the output reaches a stable single-mode state, it would tolerate certain amounts of mirror displacement and tuning current change. By estimation, the tolerance to the mirror displacement is about $0.2 \mu\text{m}$ and that to the tuning current is 0.05 mA .

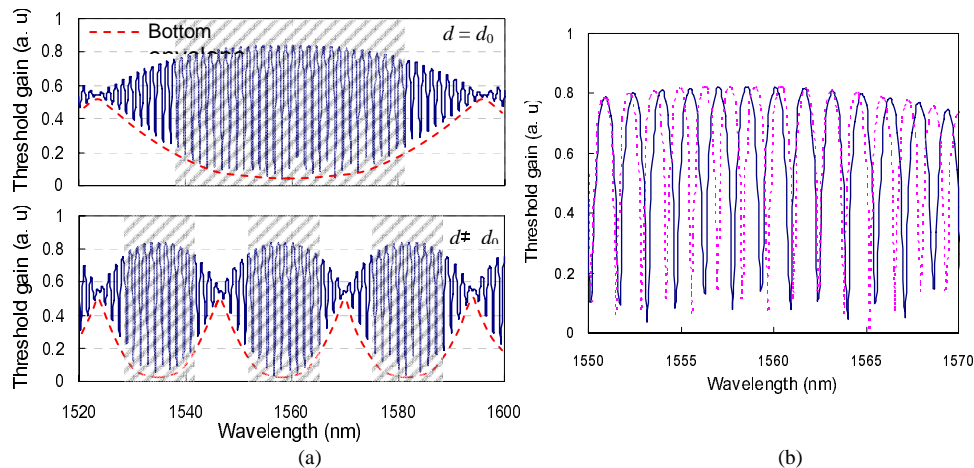


Fig. 4. Threshold gain modulation as a function of the wavelength. (a) Threshold gain versus the wavelength; and (b) shift of the threshold gain with the change of effective refractive index by the variation of the tuning current.

4. Experimental results and discussions

The overview of an assembled micromachined CCL is shown in Fig. 5 by the scanning electron micrograph. All the MEMS structures including the parabolic mirror and comb-drive actuator are fabricated by deep-reactive-ion-etching (DRIE) on a silicon-on-insulator (SOI) wafer, with a structure layer of 100- μm thick. Following the MEMS fabrication, the twin chips are assembled and soldered onto the MEMS substrate. Finally, the output fiber is inserted into and glued to the etched groove for output detection. Each chip of the twin chips is made of multiple-quantum-well InGaAsP/InP materials and has a dimension of 250 μm \times 250 μm \times 100 μm . The chip facets are normally cleaved surfaces (i.e. reflectivity $R = 29\%$). The effective reflectance of the mirror (including the optical coupling loss) is evaluated to be $R' = 0.03$ by measuring the threshold current variation while moving the curved mirror [20]. The two parts of the parabolic mirror have been designed by following $y^2 = 4px$ (where $p = 250 \mu\text{m}$). The parabolic mirror has an open angle of 60 degrees relative to the chips so as to cover 99% of the power. To improve the reflectivity of the mirror, a 0.2- μm aluminum layer is evaporated onto its surface. Moreover, to reduce the deformation of the mirror surface, a frame structure is employed to strengthen the parabolic curvature.

The position of the parabolic mirror is controlled by applying an electrostatic voltage to the comb-drive microactuator as shown in Fig. 5(b). Such adjustment ensures a precise control of the cavity gap between the two chips. The measurement results of the electro-mechanical properties of the actuators shows that a displacement of 18 μm is obtained with an applied voltage of 6 V. The displacement of the movable mirror is almost linearly increased with higher driving voltage.

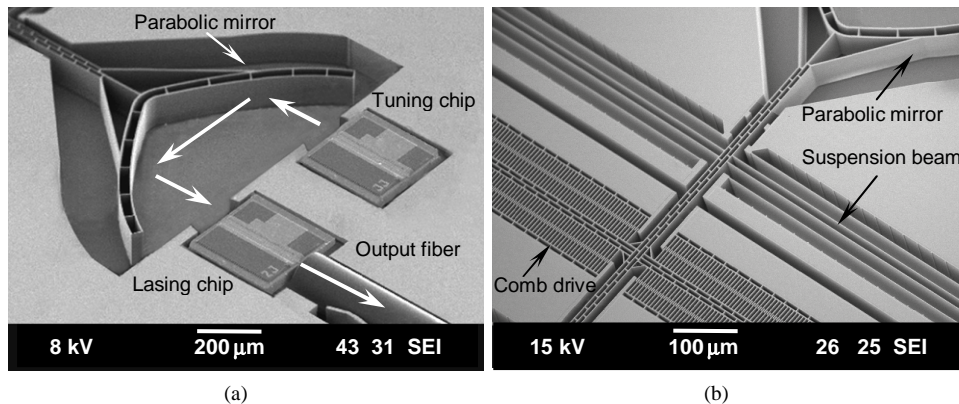


Fig. 5. Scanning electron micrograph of the micromachined coupled-cavity laser. (a) Overview of the device; and (b) close-up of the comb-drive microactuator.

Before evaluating the optical performances of the micromachined CCL, the lasing chip and the tuning chip are characterized separately. The original spectrum output of the lasing chip is shown in Fig. 6(a), with an injection current of 14.1 mA (above the threshold of 12 mA). It is observed that the single chip operates in a multi-longitudinal-mode regime. After the twin chips are assembled onto the MEMS substrate to form the micromachined CCL, the output spectrum is then characterized. During the experiment, the lasing current is kept constant at 14.1 mA while the tuning current is varied. Meanwhile, the environmental temperature is maintained at a small range 26-28 $^{\circ}\text{C}$ with an additional heat sink. The spectrum output of the laser driven by lasing current of 14.1 mA is stable and repeatable as shown in Fig. 6 (b). In addition, laser performances characterization has been carried out with and without temperature control by use of thermoelectric cooler (TEC). The output power is reduced while the output wavelength becomes unstable if the environmental temperature goes too high. The optimal cavity gap d_0 is experimentally determined by moving the parabolic

mirror back and forth while monitoring the output spectrum until a single-longitudinal-mode output is obtained. Figure 6(b) exemplifies the single-longitudinal-mode spectrum when the tuning current is 8.6 mA. It has $\lambda = 1567.7$ nm and SMSR = 24.5 dB. The gap d_0 is estimated to be 400 μm . When the cavity gap is moved away from its optimal region ($d = d_0 \pm 5$ μm), the output spectrum of the micromachined CCL becomes multi-longitudinal mode again as shown in Fig. 6(c). Such an unsuitable gap only allows the two chips work independently instead of affecting each other, even though they are optically coupled. It proves that the gap between the two chips is the dominant factor for the modes matching and wavelength selection. It is also observed that the SMSR of the single mode output of the micromachined CCL (~ 24.5 dB) is higher than the peak value (~ 17 dB) of the single chip as predicted by the analysis above.

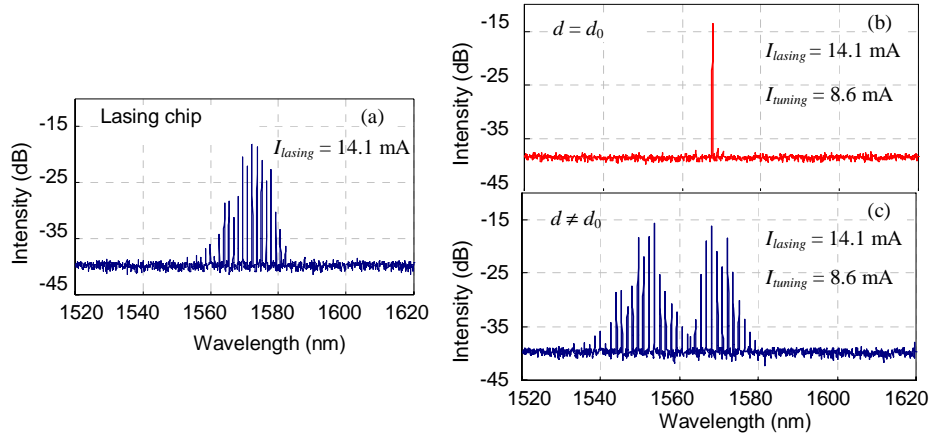


Fig. 6. Comparison of the output spectra of the micromachined CCL in different states. (a) Original multi-mode output of the single FP chip; (b) single-mode output spectrum of the micromachined CCL when the cavity gap is optimal (i.e., $d = d_0$); and (c) multi-mode spectrum of the micromachined CCL chip when the cavity gap is not optimal ($d \neq d_0$)

To study the wavelength tunability, the tuning current is varied from 5.7 to 10.8 mA. The lower limit is set at 5.7 mA because the output is not single mode if the tuning current goes lower. The upper limit of 10.8 mA is to maintain the tuning chip well below the threshold. Under the above condition, a stepwise wavelength tuning from 1540.5 to 1591.8 nm ($\Delta \lambda = 51.3$ nm) is obtained with a tuning step of 1.3 nm, at a speed of 1.2 μs . The overlapped spectra of all the possible single-mode outputs are shown in Fig. 7(a). It can be seen that the middle part of whole tuning range has high SMSR as compared to the two extremes. The middle range is replotted in Fig. 7(b), in which the output wavelength is tuned from 1551.2 to 1569.1 nm as a result of the change of tuning current over 7.05 - 8.91 mA. An average SMSR of about 22 dB is measured. Based on the experimental observation, the single mode output at any wavelength is stable when the tuning current is varied within ± 0.06 mA. On the other hand, the single mode output (driven at a constant tuning current) remains stable as long as the mirror displacement is less than 0.2 μm . Such tolerances agree well with the estimations of the tolerance mentioned above.

The output power of the CCL measures from -20 to -12 dBm. Although the lasing current can be increased to boost up the output power, such increase is limited to be less than 4 mA in order to maintain the single mode. And it is observed in this study that the output wavelength experiences a red-shift at a rate of approximately 1 nm/mA, but the tuning range and the SMSR do not change significantly. When the lasing current goes too high, the output becomes multi-longitudinal mode. To enhance the output power, it should improve the tunable laser packaging and optical system alignment, etc.

The output wavelength and SMSR as a function of the tuning current are plotted in Fig. 8. The output wavelength starts from 1540.5 nm when the tuning current is 5.7 mA. With the increase of the tuning current, the output goes to longer wavelength until 1591.8 nm. For the SMSR, it is small (~ 19.0 dB) at the beginning and increases with higher tuning current until it reaches its maximum of 25.9 dB. After that, the SMSR drops again. Such trend is reasonable since the output power and SMSR are primarily determined by the gain profile, which bends down at the two ends of the gain spectrum. It should be noted that 5 pieces of our MEMS lasers are fabricated for the experiments. Although characteristics of these laser samples (e.g. tuning current, laser current) are not exactly the same, their output performances (e.g. tuning range, SMSR) are quite similar. Moreover, all the experimental data shown here is based on the same prototype of MEMS CCL.

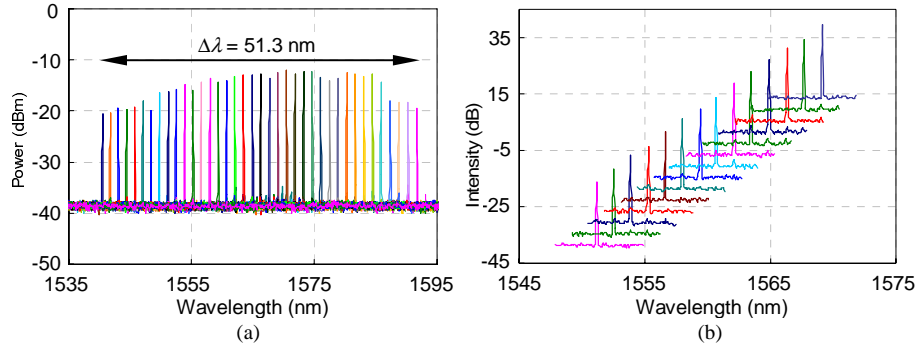


Fig. 7. Measured wavelength tunability of the integrated MEMS coupled-cavity laser. (a) Stepwise wavelength tuning from 1540.5 to 1591.8 nm with a tuning step of ~ 1.3 nm; and (b) wavelength tuning from 1551.2 to 1569.1 nm.

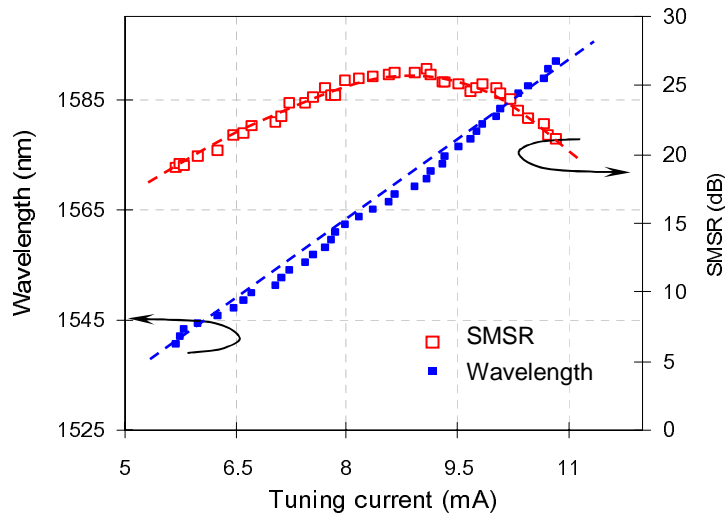


Fig. 8. Measured output wavelengths and SMSR as a function of the tuning current.

5. Conclusions

In conclusion, we have presented the design, analysis and experimental study of a micromachined coupled-cavity laser. The fabricated micromachined CCL measures a wide turning range of 51.3 nm (from 1540.5 to 1591.8 nm) while always maintaining the single longitudinal mode with a SMSR > 19.0 dB. The measured output power is about -20 to -10 dBm. The use of the adjustable air cavity gap between the cavities helps to improve the mode

selectivity and output stability. Furthermore, the speed of the wavelength switching is estimated to reach the level of nanoseconds since the tuning principle is based on the free carrier plasma effect. Both theory and experiments have shown that the wavelength tuning range of the laser can be improved by the micromachined CCL design. The use of MEMS technology not only ensures the high compactness and fine position adjustment, but also facilitates the integration of the laser chips with other optical and electronic components onto a single chip, making the micromachined CCLs promising for many applications.

Acknowledgments

This work is supported by the research grants (042 108 0097 and 042 108 0095) through the Agency for Science, Technology, and Research (A*STAR) Singapore. The authors sincerely acknowledge the collaborative partners of Institute for Infocomm Research (I²R) and Institute of Microelectronics (IME) for their supports and helps.